The Pore Structure of the $ZnO-Fe_2O_3$ Catalyst

Takeshi KOTANIGAWA and Mitsuyoshi YAMAMOTO

The Government Industrial Development Laboratory, Hokkaido, Higashi-Tsukisamu, Toyohiraku, Sapporo 061-01

(Received May 7, 1973)

With regard to the $ZnO-Fe_2O_3$ catalyst used for the selective methylation at the *ortho* position of phenol, the pore structures of the catalysts prepared by five processes were studied. The pore structures of these catalysts were determined by converting the detailed nitrogen desorption isotherm data to the pore-volume distribution. These catalysts had two types of pores, a micropore at about 20 Å and a macropore at 80 Å or more. These pores were sensitive to the sintering conditions. The micropore sizes were independent of the calcination temperature, but the macropore sizes were made proportionally larger with a rise in the calcination temperature. The macropore sizes were related to the particle sizes of the zinc ferrite formed by the solid reaction of ZnO with Fe_2O_3.

As part of a series of studies of catalysts for the synthesis of 2,6-xylenol, we previously reported that the $ZnO-Fe_2O_3$ catalyst promoted selective methylation at the *ortho* position of phenol and that simultaneously the decomposition of methanol took place as a side reaction.[1] The present catalyst was used in the above reaction without a supporter. It is, therefore, of considerable importance for the preparation of the most-favored catalyst to clarify the relations between the preparative methods of the catalyst and their pore structures. As information of this type is useful in the estimation of effective diffusion coefficients,[2] the details of pore structure have been studied on industrially-important catalysts such as alumina.[3,4] However, papers on the pore structure of the $ZnO-Fe_2O_3$ system as a catalyst for the selective methylation of phenol are not available in the literature.

We have attempt here to clarify the pore structures of $ZnO-Fe_2O_3$ catalysts prepared by various processes.

Experimental

Measurement of the Pore Structure. The adsorption-desorption isotherms were measured by using conventional volumetric equipment, as has previously been described.[5] The desorption isotherms have been used to calculate the pore-size distribution by Barrett, Joyner, and Halenda.[6] Mercury porosimeter was used for measuring the large pore-size distribution.[7] The total pore volume was measured by helium-mercury techniques.[8]

X-Ray Analysis of the Catalyst. Rigaku Denki X-ray diffractometer, with Fe$K\alpha$ radiation, was used for this purpose. Using the Scherrer equation, the crystalline sizes were calculated from the half-width of the peak of the angles (2θ) of 42°, 44.8°, and 46.1° for ferric oxide, zinc ferrite, and zinc oxide respectively. The percentage of a given crystal can be measured by calculating the area under a suitable diffraction peak and by comparing this with the corresponding area for a known sample.

Catalyst Preparation. Catalysts were prepared by the following five processes: (A) After mixing 1 mol of ferric oxide with 2 mol of zinc oxide, the mixed powder was pressed into a tablet 3 mm in diameter under pressures up to 150 kg/cm^2. (B) After the addition of 71 g of water to a mixture of 1 mol of ferric oxide and 2 mol of zinc carbonate, the mixture was kneaded for six hours at 50 °C. The paste thus prepared was forced out in a wire form 3 mm in diameter by extrusion. (C) After the addition of 67 g of water to a mixture of 1 mol of ferric hydroxide and 1 mol of zinc oxide, the mixture and the paste were treated by the method used for the (B) catalyst. (D) After the addition of 85 g of water to a mixture of 1 mol of ferric hydroxide and 1 mol of zinc carbonate, the mixture and the paste were treated by the method used for the (B) catalyst. (E) After the dissolution of 1 mol of ferric nitrate and 1 mol of zinc nitrate in water, a 14% aqueous ammonium solution was added to the solution until it gave a pH value of 6.85 at room temperature. The coprecipitate was filtered, washed several times with water, and kneaded for six hours at 50 °C. The paste was then treated by the method used for the (B) catalyst.

These wires and tablets prepared by the five processes were first heated at 150 °C for several hours to remove any moisture and then individually calcined in an electric furnace at 500, 600, 700, and 800 °C respectively for three hours with dry air being pumped into the container. They were then crushed and sieved to 12—14 mesh-size particles.

Results

Catalyst (A). The catalyst calcined at 500 °C consists of 61% ZnO, 23% Fe_2O_3, and 16% $ZnFe_2O_4$, judging from X-ray analysis. In the previous study,[1] it was confirmed through thermal analysis that the solid reaction of ZnO and Fe_2O_3 occurred at 645 °C.

Table 1. Crystalline sizes of $ZnO-Fe_2O_3$ catalyst in several preparations

Catalyst symbol	Calcination (°C)	Crystalline sizes (Å)		
		$ZnFe_2O_4$	ZnO	Fe_2O_3
A	500	367	547	249
	600	405	684	467
	700	544	628	—
	800	609	684	—
B	500	—	234	346
	600	398	261	539
	700	462	305	619
	800	820	627	—
C	500	155	596	—
	600	424	627	—
	700	557	644	—
	800	661	684	—
D	500	340	254	—
	600	358	313	—
	700	634	393	—
	800	735	547	—
E	500	169	208	—
	600	347	255	—
	700	702	460	—
	800	772	562	—

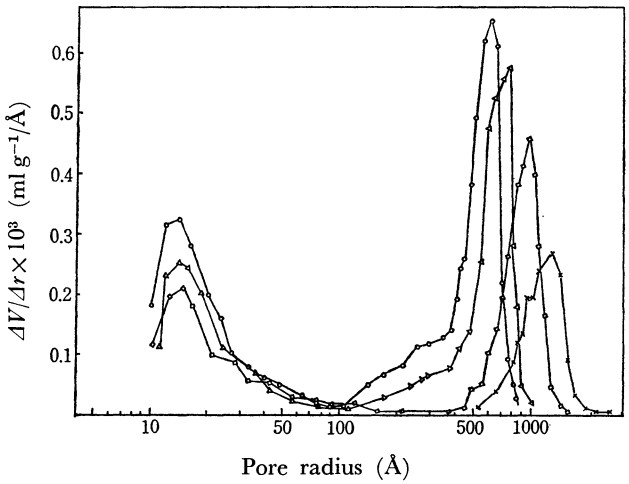

Fig. 1. Pore distribution of catalyst (A)
(-○-) at 500 °C, (-△-) at 600 °C,
(-□-) at 700 °C, (-×-) at 800 °C.

In the catalyst at 600 °C, 5% Fe_2O_3 is still present, but Fe_2O_3 is no longer present in it at 700 °C or more. The components in it are ZnO and $ZnFe_2O_4$. These crystalline sizes are shown in Table 1. The distribution of pore sizes is shown in Fig. 1. The fraction of the micropore volume per total pore volume is about 4% and is not drastically changed by the calcination temperature.

Catalyst (B). The X-ray diffraction pattern of the catalyst calcined at 500 °C does not show the line of $ZnFe_2O_4$; that is, the components in it are still ZnO and Fe_2O_3. The catalyst at 600 °C consists of 26% Fe_2O_3, 11% $ZnFe_2O_4$, and 63% ZnO. The catalyst at 700 °C consists of 24% Fe_2O_3, 14% Fe_2O_4, and 62% ZnO. However, Fe_2O_3 is no longer present in it at 800 °C. The distribution of pore sizes is shown in Fig. 2. The fraction of the micropore volume per total pore volume is 20.6% in the catalyst at 500 °C, 7.6% at 600 °C, and 6.3% at 700 °C. The micropore disappears rapidly with a rise in the calcination temperature.

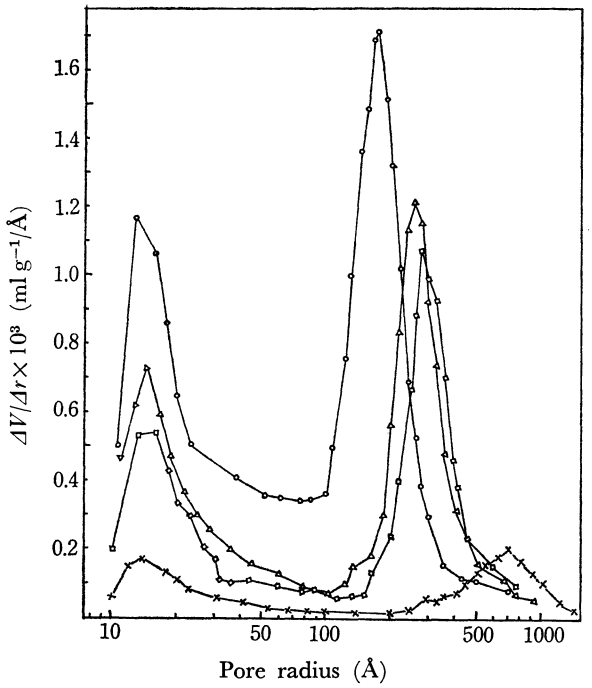

Fig. 2. Pore distribution of catalyst (B)
(-○-) at 500 °C, (-△-) at 600 °C,
(-□-) at 700 °C, (-×-) at 800 °C.

Catalyst (C). In the X-ray analysis, the only components in the catalyst are found to be ZnO and $ZnFe_2O_4$, even in the catalyst calcined at 500 °C; that is, Fe_2O_3 is not detected in any catalyst. These crystalline sizes are shown in Table 1. The distribution of pore sizes is shown in Fig. 3. The fraction of the micropore volume per total pore volume is 22.7% in the calcined at 500 °C, 14.2% at 600 °C, 8.6% at

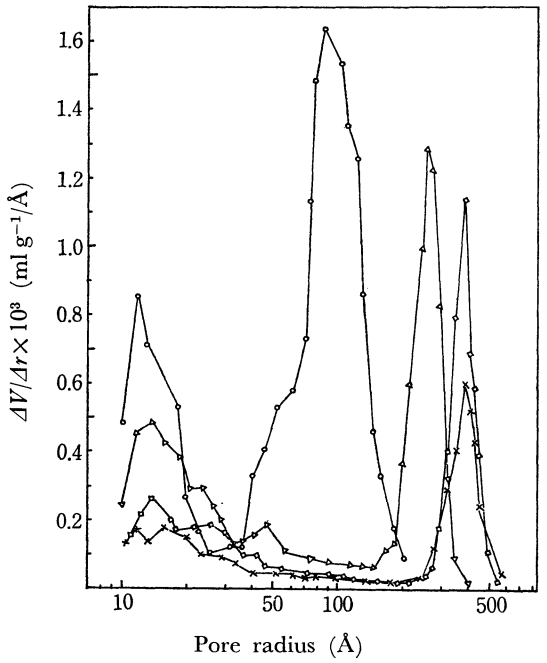

Fig. 3. Pore distribution of catalyst (C)
(-○-) at 500 °C, (-△-) at 600 °C,
(-□-) at 700 °C, (-×-) at 800 °C.

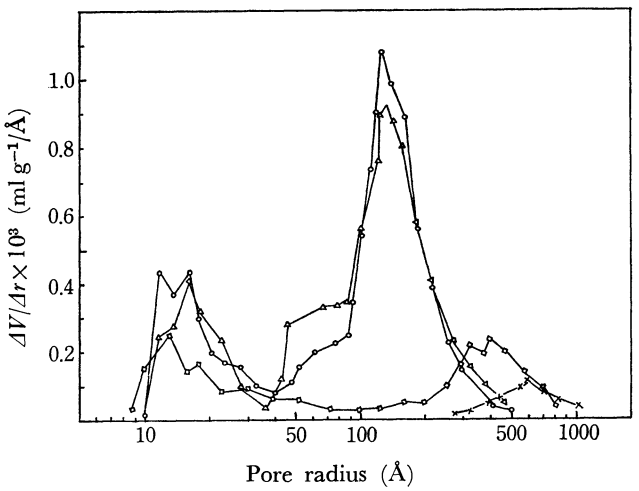

Fig. 4. Pore distribution of catalyst (D)
(-○-) at 500 °C, (-△-) at 600 °C,
(-□-) at 700 °C, (-×-) at 800 °C.

700 °C, and 8.4% at 800 °C. The disappearance of the micropore occurs rapidly with a rise in the calcination temperature.

Catalyst (D). In the X-ray analysis, the same components as in the (C) catalyst are obtained; that is, Fe_2O_3 is not detected in any catalyst. These crystalline sizes are shown in Table 1. The distribution of pore sizes is shown in Fig. 4. The fraction of the micropore volume per total pore volume is 35.1% in the catalyst calcined at 500 °C, 34.8% at 600 °C, 8.0% at 700 °C. The disappearance of the micropore occurs rapidly at 700 °C or more.

Catalyst (E). It has been reported that the formation of ferrite by the wet method depends upon pH value of the solution, but at a pH value below 10.0 the coprecipitate consists of hydroxides.[9] As the coprecipitate in the (E) catalyst is formed at a pH value of 6.85, it consists of zinc hydroxide and ferric hydroxide. In the X-ray analysis, Fe_2O_3 is not detected in any catalyst. The only components in the catalyst are ZnO and $ZnFe_2O_4$. The distribution of pore sizes is shown in Fig. 5. The fraction of the micropore volume per total pore volume is 16.6% in the catalyst calcined at 500 °C, 13.8% at 600 °C, and 6.5% at 700 °C. These crystalline sizes are shown in Table 1.

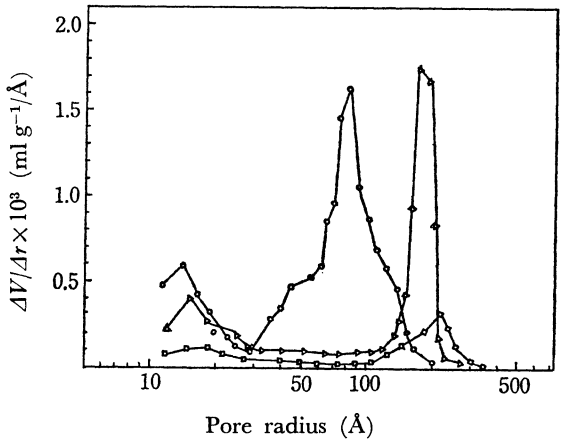

Fig. 5. Pore distribution of catalyst (E)
(-○-) at 500 °C, (-△-) at 600 °C,
(-□-) at 700 °C.

TABLE 2. PORE STRUCTURE OF ZnO-Fe_2O_3 CATALYST IN SEVERAL PREPARATIONS

Catalyst symbol	Calcination (°C)	Total pore volume (cm^3/g)	Surface area (m^2/g)	Pore radius (Å)
A	500	0.265	9.4	610
	600	0.294	7.5	710
	700	0.276	5.8	960
	800	0.192	5.3	1300
B	500	0.442	35.0	150
	600	0.418	18.8	250
	700	0.373	15.0	290
	800	0.308	5.5	700
C	500	0.190	40.4	80
	600	0.190	14.4	270
	700	0.170	8.2	380
	800	0.110	5.6	390
D	500	0.189	21.2	135
	600	0.203	19.6	140
	700	0.152	5.3	380
	800	0.100	2.3	700
E	500	0.134	36.6	85
	600	0.126	12.6	175
	700	0.058	3.3	215
	800	0.013	—	—

The pore volumes and surface areas of the present catalysts are summarized in Table 2. It may be concluded from Table 2 that the present catalysts are very sensitive to sintering.

Discussion

Three types of pores (the dehydration pore, the small interparticle pore, and the macropore (which consists of the voids between particles)) have previously been confirmed from a study of the origin of pores in the alumina.[3] However, the catalysts prepared by the five processes outlined above clearly form two types of pores, the micropore at about 20 Å and the macropore at 80 Å or more. With regard to the micropore, water and/or carbon dioxide are loosed from starting materials during the calcination. The amounts of the loss increase in the order of (D)→(B)→(E)→(C)→(A). The fraction of the micropore volume per total pore volume also corresponds to the order of the amounts of the loss of the small molecules from the starting materials. The micropore is considered to be formed by the loss of water and/or carbon dioxide from the starting materials and is considered to be a dehydration pore or a decarbonation pore.

On the other hand, the macropore becomes proportionally larger with a rise in the calcination temperature and with the growth of these crystalline sizes, as shown in Tables 1 and 2. Hence, the macropore is considered to consist of the voids between particles. In the present catalyst, zinc ferrite is formed by the

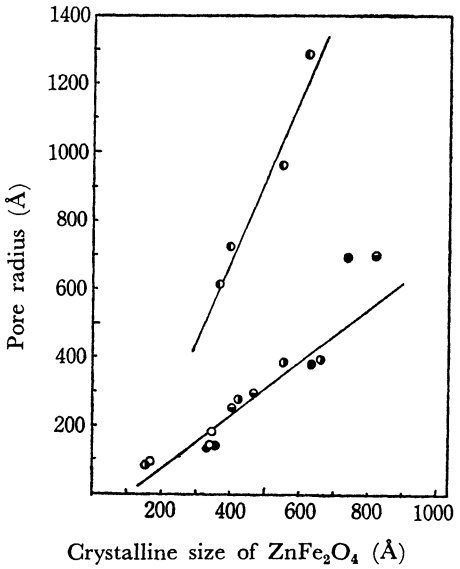

Fig. 6. Relations between pore radius and crystalline size of zinc ferrite
(-◐-) Catalyst A, (-◒-) Catalyst B, (-◑-) Catalyst C, (-●-) Catalyst D, (-○-) Catalyst E.

solid reaction of zinc oxide with ferric oxide.[1] In Table 1, the solid reaction may be seen to proceed easily in the (C), (D), and (E) catalysts, which include ferric hydroxide as a starting material. The crystalline sizes of the zinc ferrite grow considerably with a rise in the calcination temperature. Therefore, the crystalline sizes of zinc ferrite must be estimated for the formation of the macropore. The relationship between the macropore radius of these catalysts and the crystalline sizes of zinc ferrite is shown in Fig. 6. The plots of the catalysts prepared by the extrusion technique are on the same linear line, but the plot of the catalyst prepared by the tableting technique is on the other linear line. This may be expected to be due to the conditions of the preparation.

The micropore and the macropore volumes can be calculated by means of the total pore volumes and the distribution of pore sizes. From these results, the micropore may be determined to disappear mainly at temperatures below 700 °C and the macropore, to disappear suddenly at 800 °C. It may be found from the results in Table 2 that considerable decreases in the pore volume and the surface area occur with a rise in the calcination temperature. As a result, it may be concluded that the present catalyst is well crystallized and sensitive to sintering conditions.

References

1) T. Kotanigawa, M. Yamamoto, K. Shimokawa, and Y. Yoshida, This Bulletin, **44**, 1961 (1971).
2) J. M. Thomas and W. J. Thomas, "Introduction to the Principles of Heterogeneous Catalysis," Academic Press (1968).
3) M. F. L. Johnson and J. Mooi, *J. Catal.*, **10**, 342 (1968).
4) J. H. De Boer and B. C. Lippens, *ibid.*, **3**, 38 (1964).
5) H. E. Ries, M. F. L. Johnson, and J. S. Melik, *J. Phys. Colloid. Chem.*, **53**, 657 (1949).
6) E. P. Barrett, L. G. Joyner, and P. P. Halenda, *J. Amer. Chem. Soc.*, **73**, 373 (1951).
7) H. L. Ritter and L. C. Drake, *Ind. Eng. Chem. Anal. Ed.*, **17**, 782 (1945).
8) Y. Yoneda, "Shokubai Kogaku Koza," Vol. 4, Chijin Shokan, Tokyo, Vol. 4, p. 68.
9) T. Sato, M. Sugihara, and M. Saito, *Kogyo Kagaku Zasshi*, **65**, 1749 (1962).